

## DISCOVERY OF A RAPID, LUMINOUS NOVA IN NGC 300 BY THE KMTNET SUPERNOVA PROGRAM

JOHN ANTONIADIS<sup>1,2</sup>, DAE-SIK MOON<sup>3</sup>, YUAN QI NI<sup>3</sup>, DONG-JIN KIM<sup>4</sup>, YONGSEOK LEE<sup>4,5</sup>, HILDING NEILSON<sup>3</sup>

<sup>1</sup>Dunlap Institute for Astronomy & Astrophysics, University of Toronto, 50 St. George Street, Toronto, M5S 3H4, Canada

<sup>2</sup>Max-Planck-Institut für Radioastronomie, Auf dem Hügel 69, 53121, Bonn, Germany

<sup>3</sup>Department of Astronomy & Astrophysics, University of Toronto, 50 St. George Street, Toronto, M5S 3H4, Canada

<sup>4</sup>Korea Astronomy and Space Science Institute, 776 Daedeokdae-ro, Yuseong-gu, Daejeon, Korea

<sup>5</sup>School of Space Research, Kyung Hee University, Yongin 17104, Korea

### ABSTRACT

We present the discovery of a rapidly evolving transient by the Korean Microlensing Telescope Network Supernova Program (KSP). KSP is a novel high-cadence supernova survey that offers deep ( $\sim 21.5$  mag in *BVI* bands) nearly continuous wide-field monitoring for the discovery of early and/or fast optical transients. KSP-OT-201509a, reported here, was discovered on 2015 September 27 during the KSP commissioning run in the direction of the nearby galaxy NGC 300, and stayed above detection limit for  $\sim 22$  days. We use our *BVI* light-curves to constrain the ascent rate,  $-3.7(7)$  mag day<sup>-1</sup> in *V*, decay time scale,  $t_2^V = 1.7(6)$  days, and peak absolute magnitude,  $-9.65 \leq M_V \leq -9.25$  mag. We also find evidence for a short-lived pre-maximum halt in all bands. The peak luminosity and lightcurve evolution make KSP-OT-201509a consistent with a bright, rapidly decaying nova outburst. We discuss constraints on the nature of the progenitor and its environment using archival HST/ACS images and conclude with a broad discussion on the nature of the system.

*Keywords:* galaxies: individual (NGC 300) – novae, cataclysmic variables – surveys – techniques: photometric

### 1. INTRODUCTION

Over the past few years, wide-field variability surveys have significantly advanced our understanding of high-energy transients, from thermonuclear runaways and various types of supernovae (SNe) (e.g. [Rau et al. 2009](#), and references therein), to  $\gamma$ -ray ([Ackermann et al. 2013](#)) and fast radio bursts ([Thornton et al. 2013](#)).

In the optical regime, contemporary experiments are typically sensitive to two types of explosive phenomena: “local” optical transients (OTs) with small peak luminosities ( $-10 \lesssim M_b \lesssim 5$  mag), such as classical and dwarf novae, and luminous OTs with  $M_b \lesssim -15$  mag (e.g. [Chornock et al. 2013](#); [Rau et al. 2009](#); [Law et al. 2009](#), and references therein). The intermediate luminosity regime, which is as of yet poorly explored, is thought to be populated by rare cosmic explosions, such as rapid under-luminous SNe ([Drout et al. 2013](#)), accretion-induced collapse of white dwarfs (WDs; [Nomoto & Kondo 1991](#); [Metzger et al. 2009](#)), fallback SNe ([Dexter & Kasen 2013](#)), electromagnetic counterparts to compact-object mergers ([Berger et al. 2013](#)), and orphan short-GRB afterglows ([Totani & Panaitescu 2002](#)).

Exploring this parameter space is challenging for two

reasons: first, our limited understanding of the underlying physical mechanisms makes it difficult to predict characteristic observational signatures and the extent to which these OTs blend with novae and SNe populations. Second, because these events are expected to be both rapid and rare, identification requires sampling of a sufficiently large volume with high temporal resolution, thereby driving the need for deep high-cadence surveys.

High-cadence experiments are additionally motivated by outstanding questions in long-standing astrophysical problems. For instance, our understanding of “infant” thermonuclear runaways and SNe is limited, with questions regarding trigger mechanisms, shock break-out emission, ejecta masses, progenitor structure, and asymmetries still remaining ([Smartt 2009](#); [Bode & Evans 2008](#)).

Motivated by those questions, we have secured  $\sim 20\%$  of the Korea Microlensing Telescope Network (KMTNet; [Kim et al. 2016](#)) observing time through 2020 for a dedicated survey focused on infant and/or rapidly-evolving OTs, which we call the KMTNet Supernova Program (KSP; see [Moon et al. 2016](#)). KMTNet is a network of three identical 1.6-m optical telescopes located at the Cerro Tololo Inter-American Observatory in Chile, the South African Astronomical Observatory,

and the South Spring Observatory in Australia. Each telescope is equipped with a  $2^\circ \times 2^\circ$  wide-field detector, comprised of four e2v CCDs which offer  $0''.4$  pixel $^{-1}$  sampling (Kim et al. 2016). KSP is capable of providing deep ( $\lesssim 21.5$  mag $^1$ ), high-cadence continuous monitoring in  $B$ ,  $V$  and  $I$  bands (Moon et al. 2016).

In this paper we present the discovery of KSP-OT-201509a, a rapidly-evolving OT found towards a spiral arm of the Sculptor galaxy NGC 300. The transient stands out for its rapid decay rate and showcases the potential of KSP for providing well-sampled multi-color light-curves of rapidly-evolving eruptions. The paper is structured as follows. In §2, we provide a brief overview of the KSP data, and present the discovery of KSP-OT-201509a, alongside its multi-color evolution. In §3 we discuss the nature of the transient based on the lightcurve characteristics and in §4 we use HST archival images to place constraints on the progenitor of KSP-OT-201509a and its environment. Finally, we explore the ramifications of our result and conclude with a brief discussion on the prospects of the KSP in nova search in §5.

## 2. KSP-OT-201509a: DISCOVERY AND LIGHT-CURVE

Between 2015 July 1 and 2016 January 10, KSP monitored a  $15 \text{ deg}^2$  area towards the Sculptor group, including a  $4 \text{ deg}^2$  field around NGC 300 ( $d = 1.86(7) \text{ Mpc}^2$ ;  $M - m = 26.35$ ; Rizzi et al. 2006). We collected  $\sim 1300$  frames per  $BVI$  band, with a mean cadence of  $\sim 3.5$  h and an intra-day cadence ranging from  $\sim 10$  to 40 min in each filter.

The data were processed using our custom KSP pipeline which mostly relies on public software. More specifically, after acquisition flat-fielding and correction of the CCD cross talk, the data are automatically transferred to the KASI KMTNet data center for further processing. The data are then reduced using **SExtractor**<sup>3</sup> for source extraction, **SCAMP**<sup>4</sup> for astrometry and absolute photometry and **HOTPANTS**<sup>5</sup> for image subtraction. The photometric calibration is based on 4 AAVSO All-Sky Survey standard stars in the field (see Moon et al. 2016, for details). No color correction is applied. We use 60-s exposures which typically yield a limiting magnitude of  $\sim 21.5$  mag at  $S/N=5$  under  $1''.2$  seeing for point

sources. The astrometric solution, which is derived using  $\sim 10\,000$  unsaturated stars with counterparts in the second Hubble guide star catalogue (Lasker et al. 2008), accounts for scale, offset, rotation and distortion and is better than  $0''.12$ . The photon-limited astrometric precision is generally better than  $\sim 0''.5$  under  $1''.2$  seeing.

KSP-OT-201509a was discovered in the KSP data towards an NGC 300 spiral arm (Figure 1) as a faint, rapidly-evolving OT. The source first appeared on an  $I$ -band image recorded on UT 270.76<sup>6</sup> with an apparent magnitude of  $m_I = 20.7(3)$  mag, at  $(\alpha, \delta)_{J2000} = (0:55:09.422, -37:42:16.5)$ ,  $3'.373$  ( $\simeq 2$  kpc) away from the centre of the galaxy.

The original light-curve produced by our automated pipeline was contaminated by systematics, evident by the large-scale scatter ( $\sim 0.4$  mag) around the dominant decay trend. For this reason we re-analysed the data using photometry of nearby stars. More specifically, we determined the local PSF by fitting a Moffat function plus a first degree polynomial for the background to 4 bright unsaturated stars within  $3'.5$  of the transient. Apparent magnitudes were calculated by integrating the PSF over the Kron radius. Figure 2 shows the  $BVI$  light-curves of KSP-OT-201509a from first detection to its disappearance below the detection limit  $\sim 22$  days later.

### 2.1. Rising Phase

The initial phase of the transient (Figure 2), sampled on 10–12 instances per each  $BVI$  filter, is characterized by a mean ascent rate of  $-1.9(7) \text{ mag day}^{-1}$  ( $B$ ),  $-2.6(4) \text{ mag day}^{-1}$  ( $V$ ), and  $-2.5(6) \text{ mag day}^{-1}$  ( $I$ ), as determined by a linear fit to data taken prior to UT 272. However, as can be seen in Figure 2, the ascent rate seems to decrease as the transient progresses and remains practically constant in all bands after UT 270.67.

Excluding the data taken after the aforementioned time yields  $-4.0(1.0)$ ,  $-3.7(7)$  and  $-3.8(9) \text{ mag day}^{-1}$  for the mean ascent rate in  $B$ ,  $V$  and  $I$  respectively. Based on those estimates, the probability that the halt can be attributed to random noise is  $< 10^{-4}$ . Given that KSP N2015-09a re-appears brighter two nights later, we thus interpret this as evidence for a pre-maximum halt (PMH), often seen in light-curves of novae (Hillman et al. 2014).

### 2.2. Maximum and Decline Phase

KSP-OT-201509a was detected again on UT 272.33 at  $B = 18.39(1)$ , shortly after the onset of its decay phase (Figure 2). An extrapolation of our best-fit models between the rising and early decline phases suggests that

<sup>1</sup> all magnitudes reported in this work are in the Vega system

<sup>2</sup> The numbers in the parentheses are equivalent to the  $1-\sigma$  uncertainty at the last quoted digits.

<sup>3</sup> <http://www.astromatic.net/software/sextractor>

<sup>4</sup> <http://www.astromatic.net/software/scamp>

<sup>5</sup> <http://www.astro.washington.edu/users/becker/v2.0/hotpants.html>

<sup>6</sup> All times are defined relevant to Jan 1 2015.0 UT

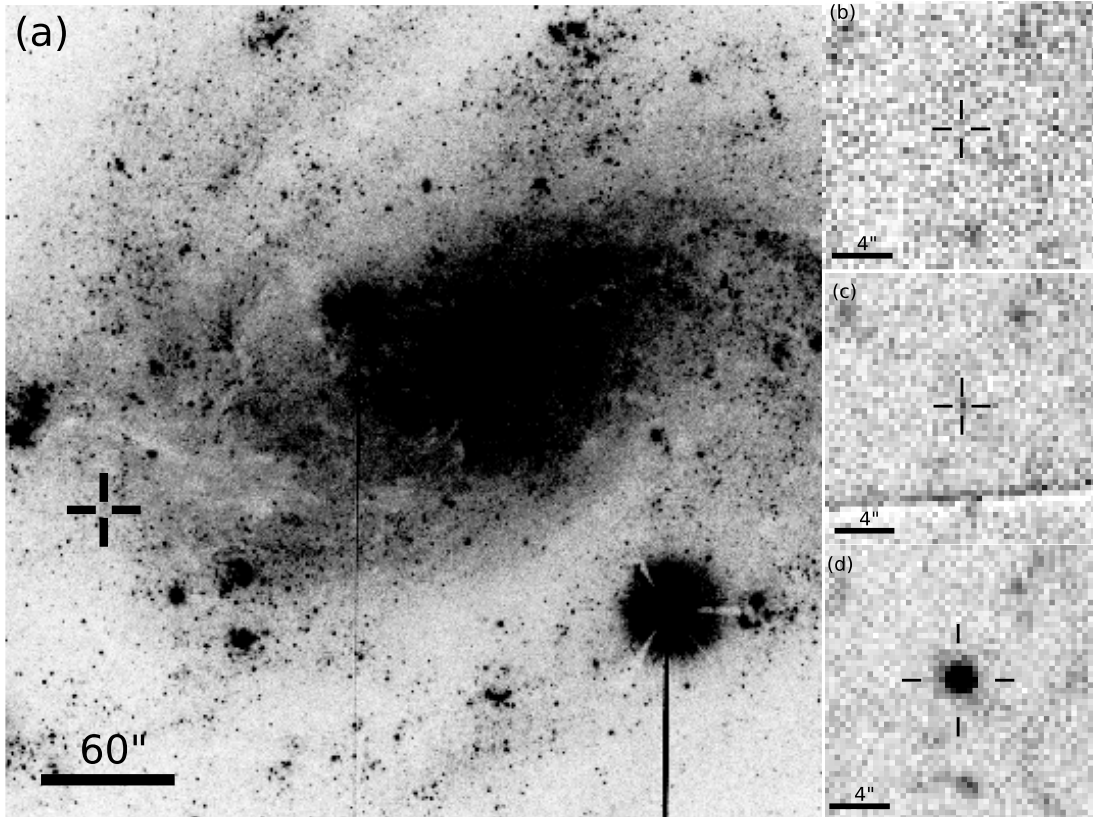


**Figure 1.** KSP-OT-201509a as recorded by KSP. Image (a) is a  $B$ -band image of NGC 300, centred at its core. North is up and east is left. Images (b) - (d) are  $I$ -band images with the same orientation. (b) is an image taken  $\sim 12$  minutes before detection and (c) is the first frame in which KSP-OT-201509a is confidently detected. Finally (d) shows the source at its maximum  $I$ -band brightness

the peak luminosity was not missed by more than  $\sim 0.6$  days. We place the maximum light between 17.9–17.6 mag, 17.1–16.7 mag, and 17.5–17.2 mag in  $B$ ,  $V$ , and  $I$  band, respectively.

Assuming the transient is indeed associated with NGC 300, the former correspond to peak absolute magnitudes between  $-8.45$  and  $-9.65$  mag. We do not account for the negligible foreground extinction ( $A_V^f = 0.03$  mag; Schlegel et al. 1998), nor for any reddening from NGC 300, which should be of the same order since the galaxy is viewed nearly edge-on.

The post-maximum evolution is characterized by a rapid decay (Figure 2). To quantify the decay rate, we adopt a decline law of the form  $F_V \propto t^{-\alpha}$ , where  $t$  is the time since maximum. For  $B$  and  $V$  we infer  $\alpha = 1.98(6)$  and  $1.84(6)$  respectively. In the  $I$  band, the decay rate evolves from  $\alpha = 1.41(6)$  at the onset of the decay phase to  $\alpha = 2.00(7)$  after  $\sim$ UT 279. From the best-fit light-curves and the times of maximum-light derived above we infer  $t_2^V = 1.7(6)$  and  $t_3^V = 3.8(7)$  days for the time

required for the  $V$ -band light-curve to fade by 2 and 3 magnitudes, respectively.

The color evolution of KSP-OT-201509a is shown in Figure 3. The decay phase starts with  $B - V \simeq 0.5$  mag and  $V - I \simeq -0.3$  mag. The color indexes then rapidly evolve to  $B - V \simeq 0.0$  mag and  $V - I \simeq 1.0$  mag in less than 1 and 4 days, respectively. Subsequently, the excess in the  $I$  band grows up to  $V - I \simeq 1.5$  mag within a few days while  $B - V$  reverts to negative values.

### 3. THE NATURE OF KSP-OT-201509a

In Section 2 we presented the lightcurve properties of KSP-OT-201509a. The peak absolute brightness inferred assuming association with NGC 300 and the rapid rising phase exclude a SN explosion or a SN impostor as the origin of the transient. Similarly, the fast post-maximum evolution disfavors an outburst on a non-degenerate star and/or a luminous red nova since those generally evolve on longer timescales (cf Pastorello et al. 2007; Williams et al. 2015, and references therein). Those features together with the presence of a multi-

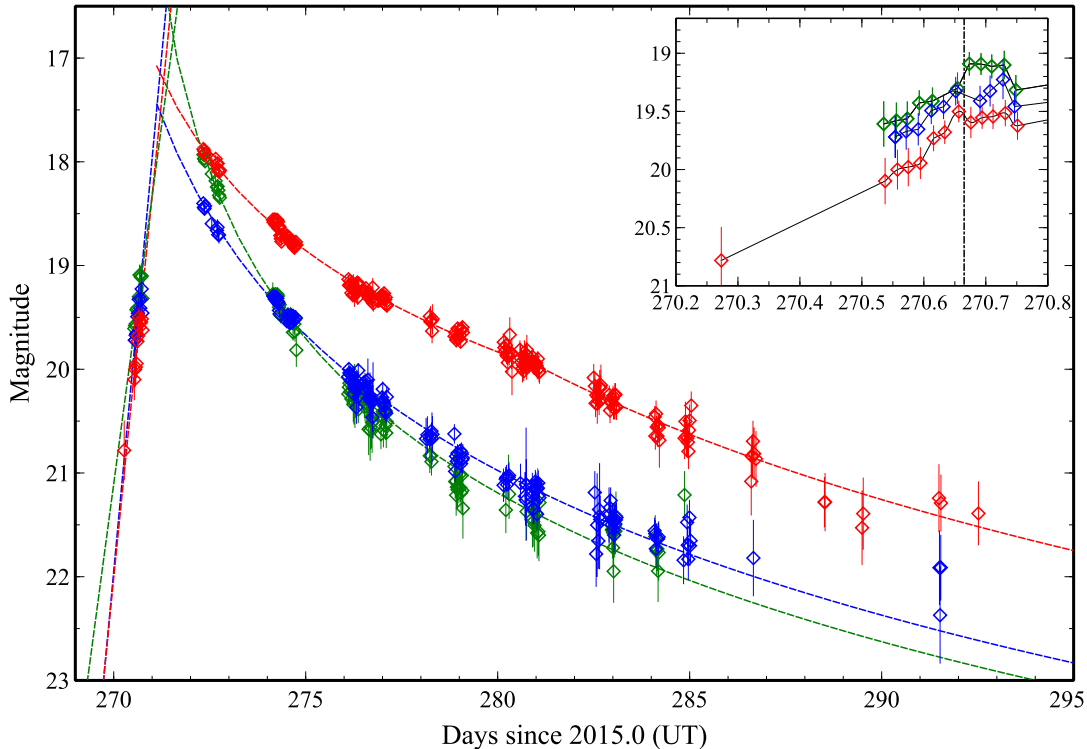


**Figure 2.** The multi-color evolution of KSP-OT-201509a. Blue, green and red points represent measurements in  $B$ ,  $V$  and  $I$  respectively. The dashed lines show the best-fit power-law decay trends ( $F_{\nu} \propto t^{-\alpha}$ ). The inset figure shows the rising phase in more detail. The vertical line at UT 270.67 indicates the approximate onset of the pre-maximum halt.

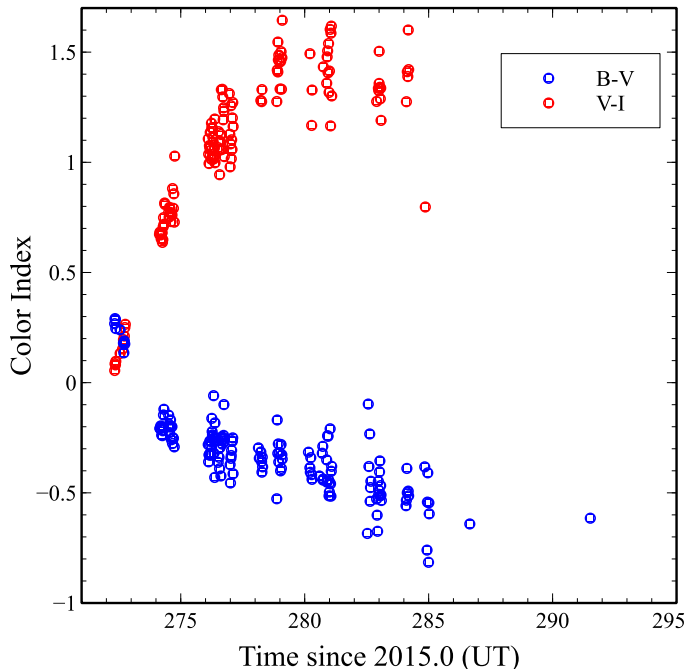


**Figure 3.** The color evolution of KSP-OT-201509a after the onset of its decay phase.

color pre-maximum halt and the smooth post-maximum evolution suggest that KSP-OT-201509a is a rapidly evolving classical nova. Indeed, the lightcurve shown

in Figure 2 shows similarities with other well-sampled fast galactic novae such as V5589 Sgr (Eyres *et al.* 2017, see §5 for a more detailed discussion). Finally, the observed peak luminosity/decline rate ratio is in good agreement with established empirical relations. For instance, the tangent maximum-magnitude/rate of decline (MMRD) relation of della Valle & Livio (1995) predicts  $M_V - 9.0(4)$  mag (here the error accounts for the uncertainty in  $t_2$  and the internal scatter of the MMRD relation). For those reasons we believe KSP-OT-201509a is indeed a fast classical nova. We adopt this classification hereafter.

#### 4. HST CONSTRAINTS ON THE PROGENITOR AND ENVIRONMENT

We analysed a set of archival HST/ACS frames towards NGC 300 obtained using the f606w and f814w filters (see Binder *et al.* 2015, for the original work). The images were taken on 2014 July 2 with 850 and 611 s exposure times, respectively.

We measured instrumental magnitudes and performed absolute calibration using DOLPHOT (Dolphin 2000). Pre-determined PSF models were used to extract instrumental magnitudes which were then corrected to infinite apertures using 12 bright isolated stars within  $1'.5$  from KSP-OT-201509a. Our absolute flux calibra-

tion is based on the most recent infinite aperture and zeropoint values for the ACS CCDs (see [Bohlin 2016](#), and references therein). We determine the  $5\sigma$  photometric limit to be  $m_{f606w} \leq 27.6$  ( $M_{f606w} \leq 0.84$ ) and  $m_{f814w} \leq 26.5$  ( $M_{f814w} \leq 0.14$ ) mag. We used the default ACS astrometric calibration (see [Anderson & King 2006](#)) which provides a distortion-free system to a level of 5 mas and then fitted for position offsets using the 4 common GSC sources nearest to KSP-OT-201509a.

Figure 4 shows the f606w image around KSP-OT-201509a, with  $0''.5$  and  $1''.0$  error circles that roughly correspond to the 68% and 95% KSP position uncertainty for a source close to the detection limit. The star nearest to the nominal KMTNet position of the source is located at  $(\alpha, \delta)_{J2000} = (0^{\text{h}}55^{\text{m}}09.422^{\text{s}}, -37^{\circ}42'16''.50)$  and has  $m_{f606w} = 26.11(9)$  and  $m_{f814w} = 25.34(10)$  mag. The brightest point-like source within the 95% error circle has  $m_{f606w} = 22.348(7)$  and  $m_{f814w} = 21.344(8)$  mag, consistent with what one would expect for a super-giant at the distance of NGC 300.

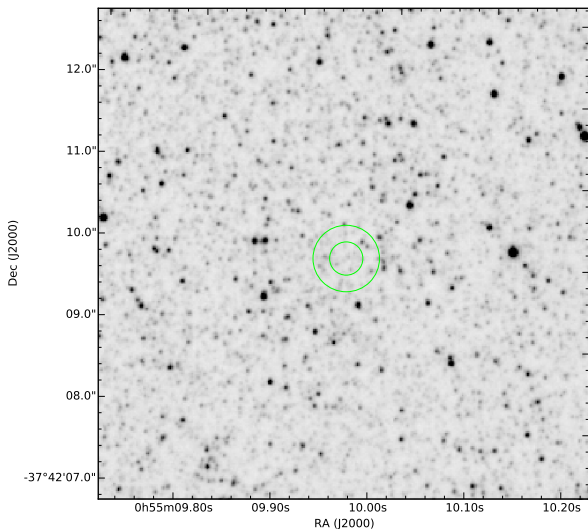


**Figure 4.** HST image of NGC 300. The green circles, centred at the position of KSP-OT-201509a represent the 1 and  $2\sigma$  astrometric uncertainties of the KSP data. The location of the brightest star is also shown.

It is unlikely that either of the HST sources inside the KMTNet error box (Figure 4) is the progenitor of KSP-OT-201509a in quiescence, as one would expect  $4 \leq M \leq 8$  for a typical main-sequence companion, which is well below the sensitivity of the HST data. The broader region, which is part of an NGC 300 spiral arm, is characterized by a large number of bright stars (with  $M_{f606w} \simeq -5$ ). This indicates that KSP-OT-201509a is likely associated with a region with high star-forming

activity.

## 5. DISCUSSION

Nova outbursts result from thermonuclear runaway eruptions on a white dwarf (WD). They occur in a binaries of the cataclysmic-variable type, in which matter is accreted from a non-degenerate companion (e.g. [Darnley et al. 2012](#)). Material accumulating on the WD surface eventually causes the envelope to become electron degenerate, leading to a runaway thermonuclear flash which ultimately gives rise to the nova phenomenon.

It is well established, both theoretically and observationally, that nova time scales, amplitudes and recurrence rates depend sensitively on the WD mass, mass-accretion rate, envelope mass, companion type and wind power ([Yaron et al. 2005](#)). With few exceptions, bright and fast novae (hereafter FNe) occur in systems with massive WDs and high mass-accretion rates between  $\dot{M}_{\text{acc}} \simeq 10^{-8}$  and  $10^{-4} M_{\odot} \text{ yr}^{-1}$  ([Priyalnik & Kovetz 1995](#); [Yaron et al. 2005](#)).

FNe rising phases last up to few days (e.g. [Kato et al. 2009](#); [Strope et al. 2010a](#)). During this time, the effective temperature increases dramatically (initially at constant radius) causing the surface brightness to rise by 10–20 magnitudes. Recent studies find no strong correlation between the ascent rate and peak brightness (e.g. [Cao et al. 2012](#)), although no safe conclusions can be drawn from existing data. In addition, because of the rapid evolution time scales, very few infant FNe have been sampled with sufficient temporal cadence in multiple band to probe the underlying eruption mechanism in detail.

The work presented here provides an unprecedented multi-color view of an early FN eruption phase. We find that the brightness of KSP-OT-201509a increases at  $-3.7 \text{ mag day}^{-1}$  in  $V$ , indicating a total rising-phase duration between  $\sim 2.5$  and 5 days.

In addition, our data provide evidence for a short-lived pre-maximum halt (PMH) after UT 270.67 (Figure 2). While PMHs have been observed both in slow and fast novae (see [Hounsell et al. 2010, 2016](#), and references therein), it is yet unclear if they reflect an intrinsic change of the WD.

For instance, some early studies suggest that they may be triggered by an external condition such as a sudden enhancement of mass loss from the donor. More recent theoretical work based on detailed 1D simulations ([Hillman et al. 2014](#)) finds that PMHs are explained naturally by a decrease in the convection-transport efficiency. The rise to peak brightness continues after the opacity decreases for radiation-transport to take over at the onset of the mass-loss phase. In KSP-OT-201509a one sees that the color index remains constant during the PMH and later evolves rapidly between the late-rise and early-

decline phases (see Figures 2 and 3). This is consistent with a transition in the emission mechanism expected in the latter scenario (see below).

In the early decline phase it is expected that the continuum spectrum is dominated by free-free scattering above the optically-thick photosphere. For the idealized case of pure optically-thin thermal Bremsstrahlung, Kato *et al.* (2009) find a universal decay law,  $F_\nu \propto t^{-1.75}$ , which matches well the observed light-curve of KSP-OT-201509a (§ 2). This in turn suggests that the transient evolution depends strongly on the wind rate and velocity, and less so on the WD mass (Kato *et al.* 2009, and references therein). At later phases, especially after UT 276.9, the transition to a steeper *I*-band decline rate suggests the presence of an additional thermal emission component (Hachisu & Kato 2016) which may indicate the presence of additional emission components, for instance the formation of a dust shell.

Considering that no spectroscopic information is available for KSP-OT-201509a, we resort to other historical FNe and theoretical studies to draw further conclusions on the WD mass and the nature of the donor star as below. Examples of well-studied bright ( $-8.5 \leq M_V \leq -10.5$ ) FNe in the Galaxy include (Strope *et al.* 2010b) V838 Her ( $t_2 \simeq 1$  day), V1500 Cyg ( $t_2 \simeq 2$  days), V2275 Cyg ( $t_2 \simeq 3$  days) and more recently V2491 Cyg ( $t_2 \simeq 2$  days; Hounsell *et al.* 2016) and V5589 Sgr ( $t_2 \simeq 2.5$  days Eyres *et al.* 2017). Spectra from the early eruption phases for these FNe indicate terminal wind velocities of  $\sim 1000$  to  $3000$  km s $^{-1}$ . In almost all cases, FNe are associated with massive ( $\geq 1 M_\odot$ ) WDs and a total wind mass-loss of few times  $10^{-6} M_\odot$ . Given

the observational similarities between KSP-OT-201509a and these FNe, we therefore conclude that the former most likely also hosts a massive WD of  $\geq 1 M_\odot$ .

The discovery of KSP-OT-201509a in an early phase and dense multi-color monitoring of its light-curve through its entire eruption demonstrates the potential of KSP to provide an unprecedented view of novae and related phenomena. Based on the KSP early performance and sensitivity so far, we expect to detect several tens of classical novae as well as other transients, including infant and nearby SNe (Moon *et al.* 2016).

We thank the anonymous referee for the useful suggestions. This research has made use of the KMTNet system operated by the Korea Astronomy and Space Science Institute (KASI) and the data were obtained at three host sites of CTIO in Chile, SAAO in South Africa, and SSO in Australia. KSP is partly supported by an NSERC Discovery Grant to DSM. JA is a Dunlap Fellow at the Dunlap Institute for Astronomy and Astrophysics at the University of Toronto. The Dunlap Institute is funded by an endowment established by the David Dunlap family and the University of Toronto. We have made extensive use of NASA's Astrophysics Data System. This research made use of Astropy, a community-developed core Python package for Astronomy.

*Facility:* KMTNet, HST(WFPC2)

*Software:* Astropy

## REFERENCES

- Ackermann, M., Ajello, M., Asano, K., *et al.* 2013, *ApJS*, 209, 11  
 Anderson, J., & King, I. R. 2006, *Instrument Science Report ACS 2006-01*, 34 pages, 1, 1  
 Berger, E., Fong, W., & Chornock, R. 2013, *ApJ*, 774, L23  
 Binder, B., Gross, J., Williams, B. F., & Simons, D. 2015, *MNRAS*, 451, 4471  
 Bode, M. F., & Evans, A. 2008, *Classical Novae*  
 Bohlin, R. C. 2016, *AJ*, 152, 60  
 Cao, Y., Kasliwal, M. M., Neill, J. D., *et al.* 2012, *ApJ*, 752, 133  
 Chornock, R., Berger, E., Rest, A., *et al.* 2013, *ApJ*, 767, 162  
 Darnley, M. J., Ribeiro, V. A. R. M., Bode, M. F., Hounsell, R. A., & Williams, R. P. 2012, *ApJ*, 746, 61  
 della Valle, M., & Livio, M. 1995, *ApJ*, 452, 704  
 Dexter, J., & Kasen, D. 2013, *ApJ*, 772, 30  
 Dolphin, A. E. 2000, *PASP*, 112, 1383  
 Drout, M. R., Soderberg, A. M., Mazzali, P. A., *et al.* 2013, *ApJ*, 774, 58  
 Eyres, S. P. S., Bewsher, D., Hillman, Y., *et al.* 2017, *MNRAS*, 467, 2684  
 Hachisu, I., & Kato, M. 2016, *ArXiv e-prints*, arXiv:1602.01195  
 Hillman, Y., Prialnik, D., Kovetz, A., Shara, M. M., & Neill, J. D. 2014, *MNRAS*, 437, 1962  
 Hounsell, R., Bode, M. F., Hick, P. P., *et al.* 2010, *ApJ*, 724, 480  
 Hounsell, R., Darnley, M. J., Bode, M. F., *et al.* 2016, *ApJ*, 820, 104  
 Kato, M., Hachisu, I., & Cassatella, A. 2009, *ApJ*, 704, 1676  
 Kim, S.-L., Lee, C.-U., Park, B.-G., *et al.* 2016, *Journal of Korean Astronomical Society*, 49, 37  
 Lasker, B. M., Lattanzi, M. G., McLean, B. J., *et al.* 2008, *AJ*, 136, 735  
 Law, N. M., Kulkarni, S. R., Dekany, R. G., *et al.* 2009, *PASP*, 121, 1395  
 Metzger, B. D., Piro, A. L., Quataert, E., & Thompson, T. A. 2009, *ArXiv:908.1127*, arXiv:0908.1127  
 Moon, D.-S., Kim, S. C., Lee, J.-J., *et al.* 2016, in *SPIE Astronomical Telescopes+ Instrumentation*, International Society for Optics and Photonics, 99064I–99064I  
 Nomoto, K., & Kondo, Y. 1991, *ApJ*, 367, L19  
 Pastorello, A., Smartt, S., Mattila, S., *et al.* 2007, *Nature*, 447, 829  
 Prialnik, D., & Kovetz, A. 1995, *ApJ*, 445, 789  
 Rau, A., Kulkarni, S. R., Law, N. M., *et al.* 2009, *PASP*, 121, 1334  
 Rizzi, L., Bresolin, F., Kudritzki, R.-P., Gieren, W., & Pietrzyński, G. 2006, *ApJ*, 638, 766

- Schlegel, D. J., Finkbeiner, D. P., & Davis, M. 1998, *ApJ*, 500, 525
- Smartt, S. J. 2009, *ARA&A*, 47, 63
- Strope, R. J., Schaefer, B. E., & Henden, A. A. 2010a, *AJ*, 140, 34
- . 2010b, *AJ*, 140, 34
- Thornton, D., Stappers, B., Bailes, M., et al. 2013, *Science*, 341, 53
- Totani, T., & Panaitescu, A. 2002, *ApJ*, 576, 120
- Williams, S. C., Darnley, M. J., Bode, M. F., & Steele, I. A. 2015, *ApJ*, 805, L18
- Yaron, O., Prialnik, D., Shara, M. M., & Kovetz, A. 2005, *ApJ*, 623, 398